Supporting Information for

Quantifying Carbon Cycling across the Groundwater–Stream–Atmosphere Continuum Using High-Resolution Time Series of Multiple Dissolved Gases

Chuan Wang [a, b, c], Matthias S. Brennwald [c], Yueqing Xie [a, b, *], James L. McCallum [d], Rolf Kipfer [c, e, f], Xin Dai [a, b], and Jichun Wu [a, b]

[a] Key Laboratory of Surficial Geochemistry, Ministry of Education, School of Earth Sciences and Engineering, Nanjing University, Nanjing 210023, China

[b] Frontiers Science Center for Critical Earth Material Cycling, Nanjing University, Nanjing 210023, China

[c] Department of Water Resources and Drinking Water, Eawag, Swiss Federal Institute of Aquatic Science and Technology, Dübendorf 8600, Switzerland

[d] School of Earth Sciences, University of Western Australia, Perth 6009, Western Australia, Australia

[e] Department of Environmental System Sciences, Institute of Biogeochemistry and Pollutant Dynamics, ETH Zürich, Zürich 8092, Switzerland

[f] Department of Earth Sciences, Institute of Geochemistry and Petrology, ETH Zürich, Zürich 8092, Switzerland

[*]Corresponding author: Yueqing Xie (yxie@nju.edu.cn)

Contents of this file

Text S1, Field measurement description; Text S2, Numerical model for dissolved gas time series in the stream; Figure S1, Geographical location; Figure S2, Diurnal variations in water levels in the stream and the groundwater; Figure S3, Measured dissolved gas concentrations in different endmembers; Figure S4, Comparison of Ar, He, and Kr concentrations in different endmembers; Figure S5, Scatter plot of the difference between measured and equilibrium noble gases and N_2 concentrations.

Text S1. Field measurement description

We installed one piezometer (diameter: 7 cm, screen: 8 cm, depth: 40 cm) at the streambed for sampling streambed groundwater and three piezometers (diameter: 5 cm, depth: 2 m, screen length: 1.5 m) at the riparian zone for sampling riparian groundwater (see Figure 1a). Submersible pumps were used to extract the stream water and groundwater to the constructed field camp for measurement. Our high-resolution time series measurement lasted five days and continued from 0:00 on 28th November to 0:00 on 3rd December 2021. We used the portable and autonomous gas-equilibrium membrane-inlet mass spectrometry (GE-MIMS, Gasometrix GmbH, Switzerland) to continuously analyze dissolved ^{40}Ar, ^{4}He, ^{84}Kr, CO_2, CH_4, and O_2 concentrations (see Brennwald, et al. [1] for details). Two standard gas mixtures (mixture I: 2057 ppm CO_2 in N_2 background, mixture II: 20.1 ppm CH_4 in N_2 background, Air Liquide) were used to calibrate CO_2 and CH_4, respectively, while ambient air was used to calibrate ^{40}Ar, ^{4}He, ^{84}Kr, and O_2 as suggested by Brennwald, et al. [1]. In addition, two water level loggers were deployed in the stream and the streambed piezometer for in-situ water temperature measurements at 10 min intervals. We also installed a weather station to record the local solar radiation and air temperature during the investigation (see Figure 1c).

Text S2. Numerical model for dissolved gas time series in the stream

The concentrations of dissolved gases in the streams are often highly variable due to the gas exchanges with the adjacent groundwater and atmosphere, the effect of changing stream levels, and the biogeochemical reactions within the stream channels. By considering the gas input from groundwater, gas exchange at the stream–atmosphere interface, the varying stream levels, and the biogeochemical reactions in the stream, the mass balance of dissolved gases in a specific stream reach can be expressed as (also see the conceptual model in Figure 1b)

$$\frac{d\left(wzlC_i\right)}{dt} = Q_{up}C_i + v_v wlC_{v,i} + 2v_l zlC_{l,i} + k_i wl(C_{eq,i} - C_i) - (Q_{up} + Q_{gw})C_i + wlR_i \qquad \text{(S1)}$$

$$k_i = k_{600}\left(\frac{Sc_i(T)}{600}\right)^{-0.5} \qquad \text{(S2)}$$

$$Q_{gw} = v_v wl + 2v_l zl \qquad \text{(S3)}$$

where C_i, $C_{v,i}$, $C_{l,i}$, and $C_{eq,i}$ are the stream concentration, the vertical groundwater concentration, the lateral groundwater concentration, and the atmospheric equilibrium concentration of gas *i*, respectively. w, z, and l are the stream width, the depth, and the length, respectively. Q_{up} and Q_{gw} are the upstream flow rate and the total groundwater discharge rate. v_v, v_l, and k_i are the vertical groundwater discharge velocity, the lateral groundwater velocity, and the gas transfer velocity, respectively. k_{600} is the gas transfer velocity with a Schmidt number of 600 and Sc_i is the Schmidt number of gas *i* and depends on temperature.

By assuming the rectangle stream channel conditions, only z and C_i are varied with time, and the left side of Equation S1 becomes

$$\frac{d\left(wzlC_i\right)}{dt} = wlC_i\frac{dz}{dt} + wzl\frac{dC_i}{dt} \tag{S4}$$

Substituting Equations S2, S3 and S4 into S1 and dividing wzl for both sides, we can get the following equation:

$$\frac{dC_i}{dt} = \frac{v_v(C_{v,i} - C_i)}{z} + \frac{2v_l(C_{l,i} - C_i)}{w} + \frac{k_i(C_{eq,i} - C_i)}{z} - \frac{C_i}{z}\frac{dz}{dt} + \frac{R_i}{z} \tag{S5}$$

The first and second terms on the right side of Equation S1 represent the net mass inflows from vertical and lateral groundwater discharges, respectively. We assume the lateral groundwater discharges from the left and right sides of the riverbank are identical. The third term is the gas exchange at the stream–atmosphere interface. The fourth term represents the effect of changes in the stream level, and can be eliminated under a steady-state flow condition (i.e., the stream level is constant). The fifth term is the impact of biogeochemical reaction (for noble gases, R_i = 0).

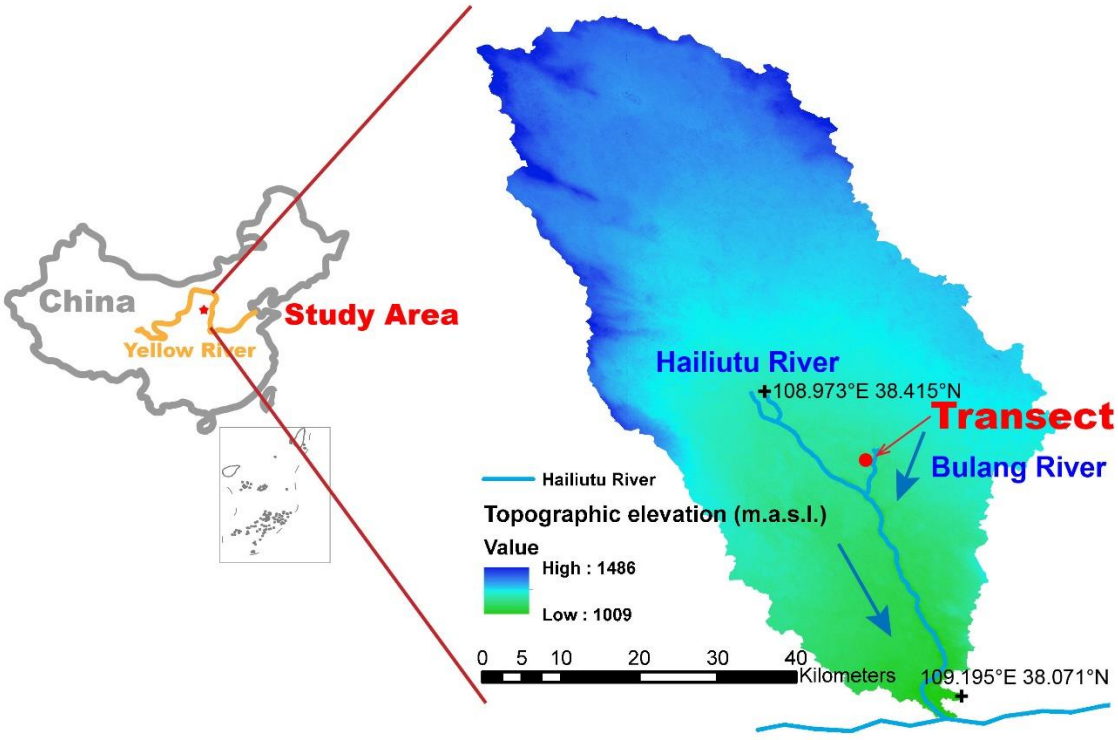

Fig. S1. Geographical locations of the Hailiutu River catchment and the studied transect.

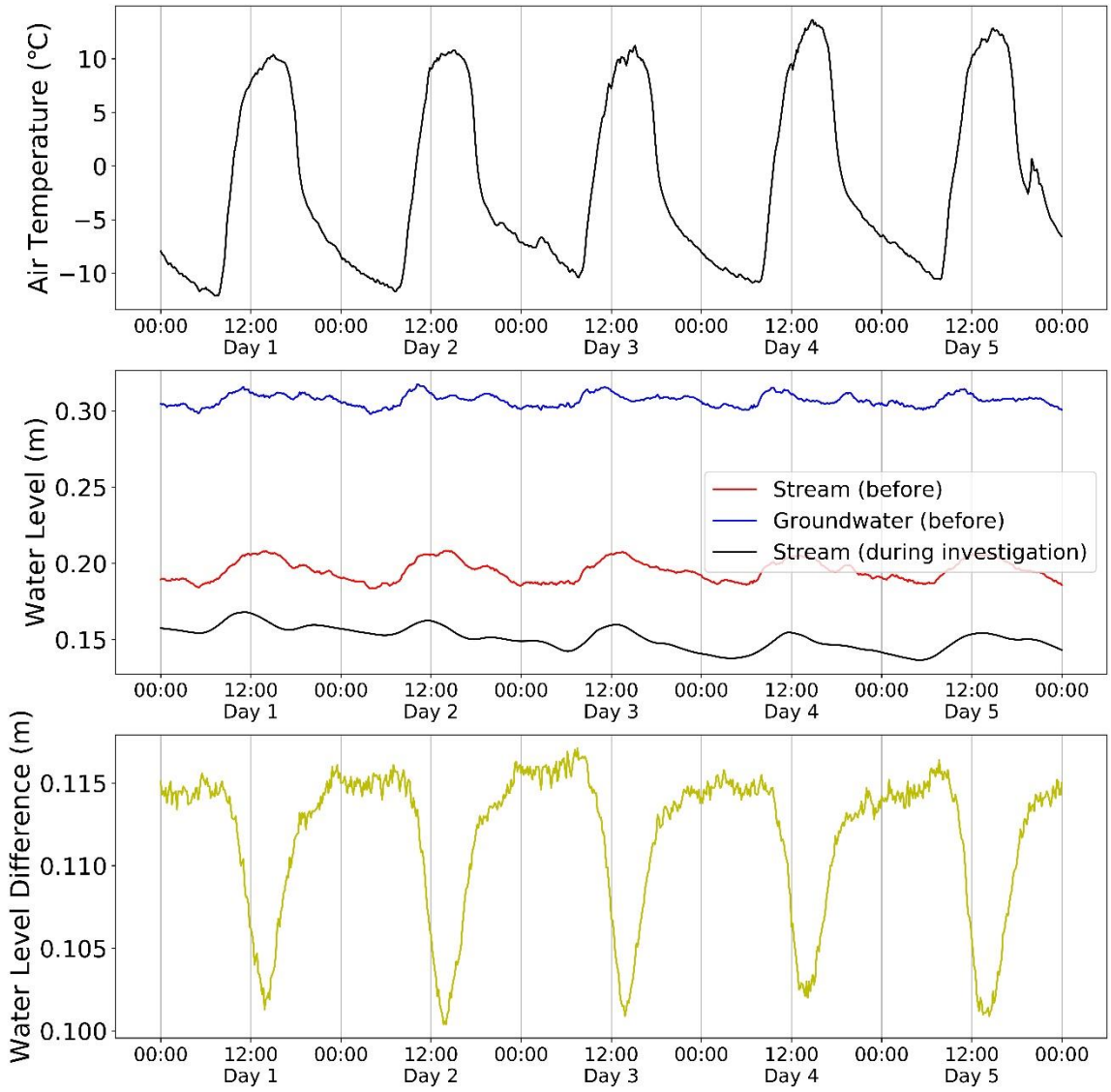

Fig. S2. Diurnal variations in water levels in the stream and the groundwater. Since groundwater level measurements were not taken during the investigation due to the need for pumping, the data (except black line in the middle panel) presented is from several days before the investigation (13-17th November 2021). The increases in water levels during the day and decreases at night were likely caused by diurnal freezing and thawing in the upstream area, given the headwater nature of the study site. The 10% variation in water level difference between the groundwater and stream suggests a diurnal fluctuation in groundwater discharge.

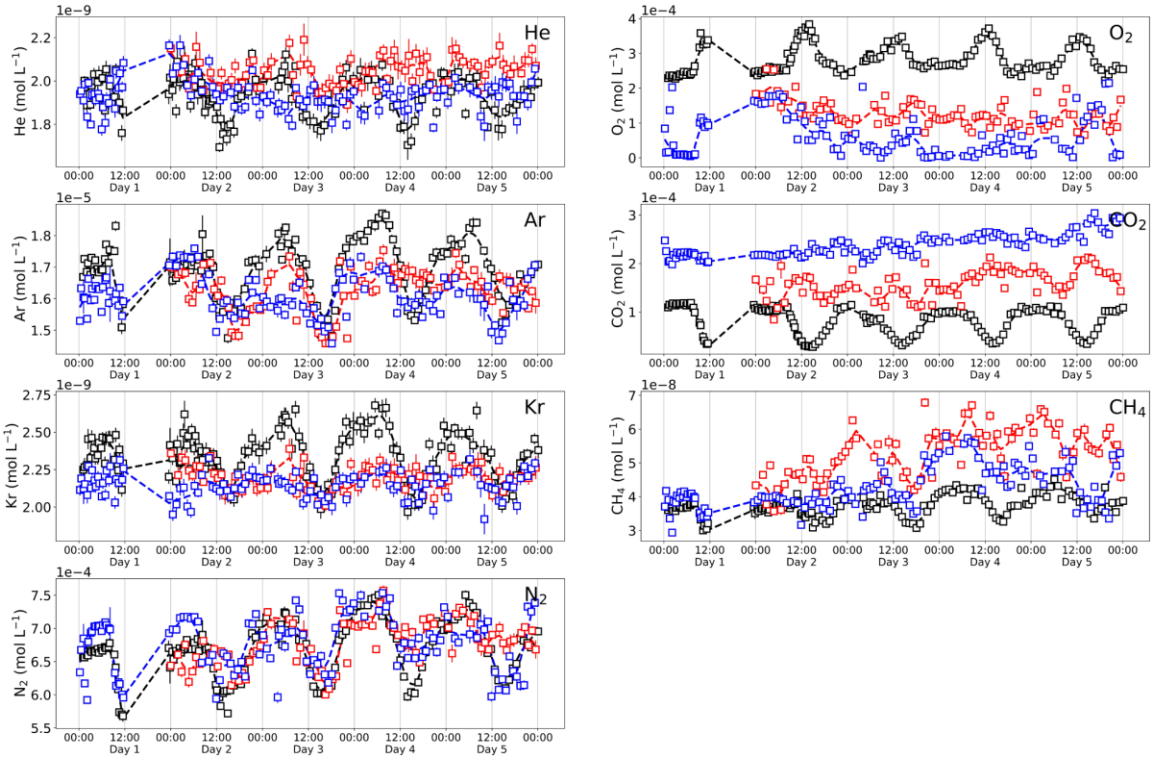

Fig. S3. Measured dissolved gas concentrations in the stream (black dots, C_i), the streambed water (red dots, $C_{v,i}$), and the riparian groundwater (blue dots, $C_{l,i}$).

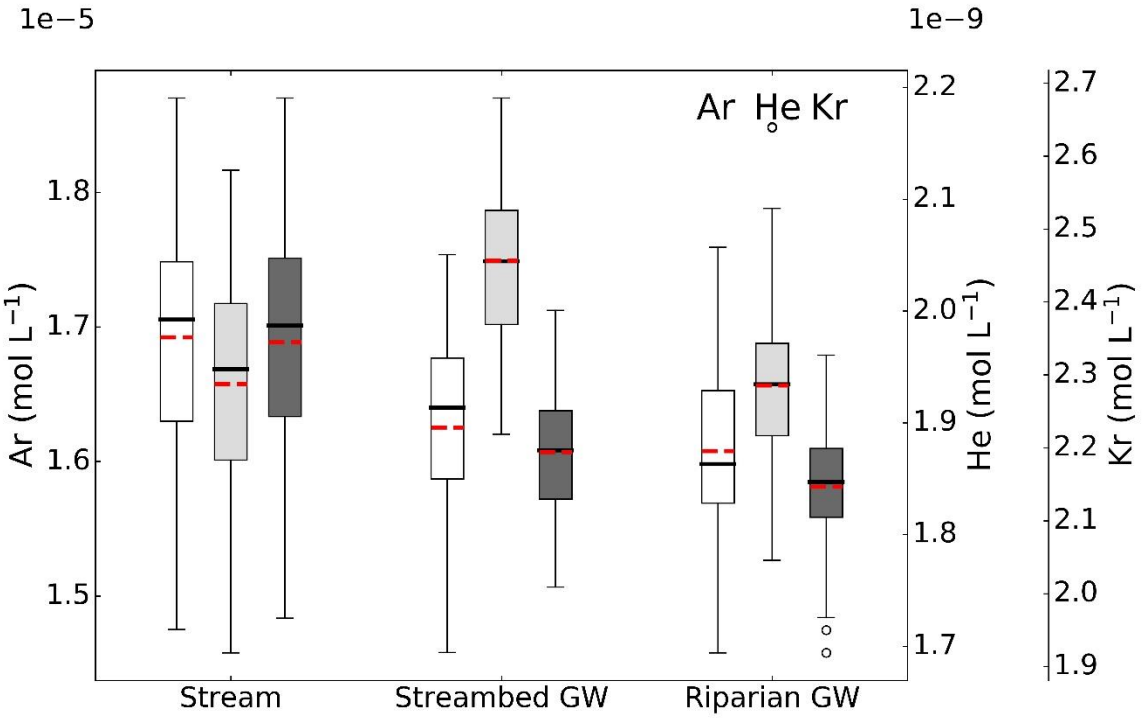

Fig. S4. Comparison of time series of Ar, He, and Kr concentrations in the stream water (C_i), streambed water ($C_{v,i}$), and riparian groundwater ($C_{l,i}$). This comparison reveals that stream has lower He, and higher Ar and Kr concentrations (C_i) than the boundary conditions (i.e., $C_{v,i}$ and $C_{l,i}$).

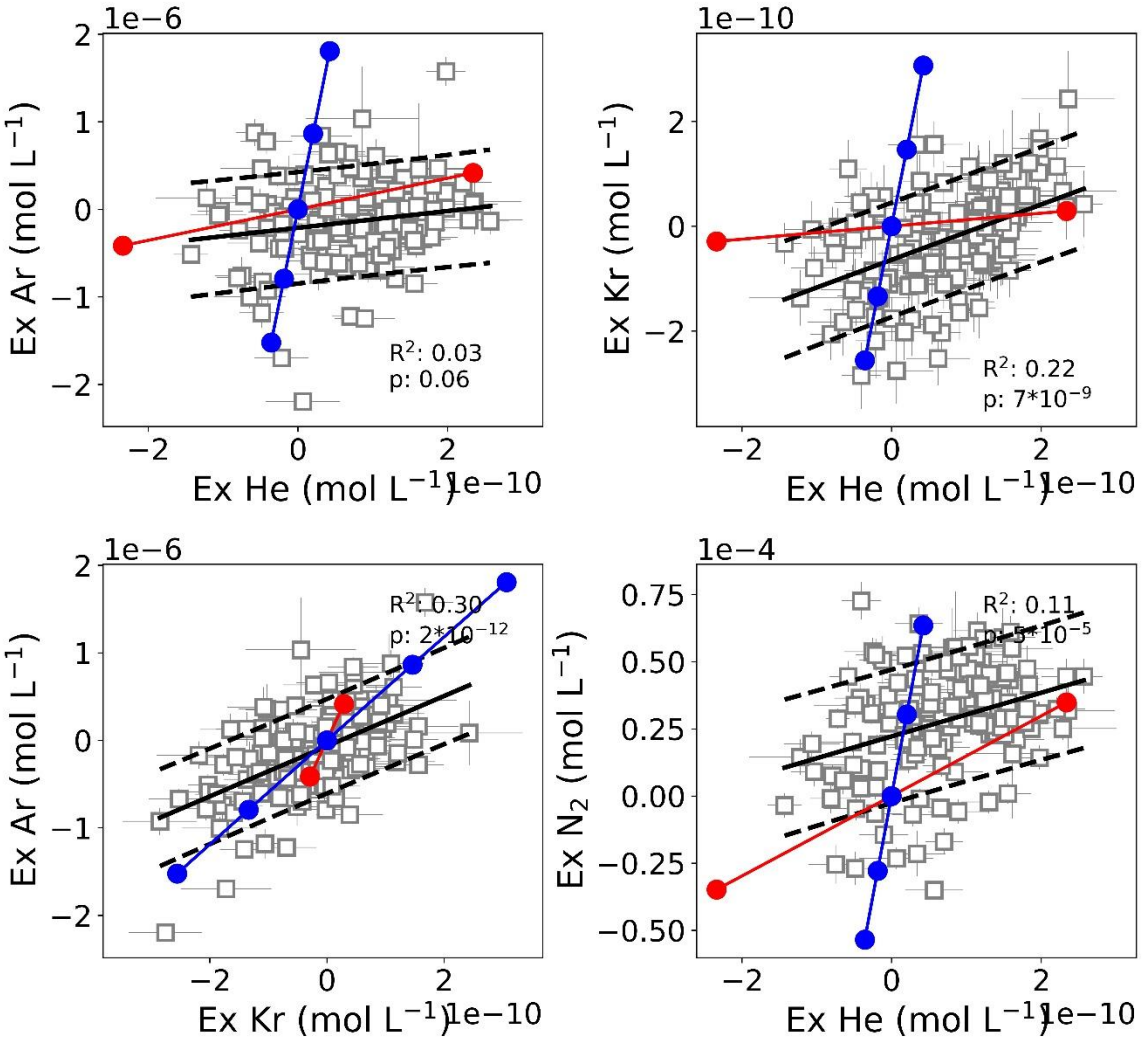

Fig. S5. Scatter plot of the difference between measured and equilibrium noble gases and N_2 concentrations (measured–equilibrium). Black lines are linear regression and 90% confidence intervals, and red dots are the air-like excess air ($–1.0*10^{-3}$, 0, $1.0*10^{-3}$ cm^3 STP g^{-1}). Blue line represents the influence of temperature changes (2, 4, 6, 8, 10 ℃).

References

(1) Brennwald, M. S.; Schmidt, M.; Oser, J.; Kipfer, R., A Portable and Autonomous Mass Spectrometric System for On-Site Environmental Gas Analysis. *Environ. Sci. Technol.* **2016,** *50*, (24), 13455-13463.